Journal of Catalysis **204,** 200–208 (2001)
doi:10.1006/jcat.2001.3392, available online at http://www.idealibrary.com on IDEAL®

Catalytic Hydrolysis of Dichlorodifluoromethane over Nanosized Titania-Supported Titanyl Sulfate

Xingyi Deng, Zhen Ma, Yinghong Yue, and Zi Gao[1]

Department of Chemistry, Fudan University, Shanghai 200433, People's Republic of China

Received May 15, 2001; revised August 14, 2001; accepted August 14, 2001

Catalytic hydrolysis of CCl_2F_2 in the presence of water vapor and air was studied over a series of metal sulfates. $TiOSO_4$ displayed the highest activity among these sulfates, over which the conversion of CCl_2F_2 reached 100% at 310°C. Supporting $TiOSO_4$ on nanosized anatase TiO_2 further increased its activity. CCl_2F_2 decomposed completely on the supported catalysts at 260–265°C. The effects of $TiOSO_4$ loading, calcination temperature, and properties of support on activity of the supported catalysts were investigated. The activity of this type of catalyst correlates well with its specific surface area and the amount of medium-strong acid sites on the surface. No deactivation of the catalyst was observed during 360 h on stream at 260°C. CO was not detected in the effluent gas and the selectivity to $CClF_3$ in the product remained lower than 0.5%.

Key Words: **chlorofluorocarbons; CCl_2F_2 hydrolysis; metal sulfates; titanyl sulfate; nanosized anatase TiO_2 support.**

INTRODUCTION

The ozone layer acts as an atmospheric shield that protects life on the earth against ultraviolet radiation from the sun. In the past three decades, it has become very clear that this fragile shield was gradually depleted by chlorofluorocarbons (CFCs) diffused into the stratosphere (1), which leads to a variety of adverse effects such as an increase in the incidence of skin cancer. The ultimate solution of this problem is to stop the production and use of CFCs. In fact, the Montreal Protocol, an international treaty to phase out and control CFCs, was signed in 1987 and presently has 163 signatories. However, there are still 2.25 million-ton of CFCs all over the world and numerous air-conditioning systems are still using them as coolants. Therefore, finding a practical way to eliminate the CFC pollutants or ultimately to destroy all the existing CFCs is urgently required. There are a dozen CFC destruction techniques such as incineration (2), cement kiln (3), plasma (4), supercritical water (5), electrochemical decomposition (6, 7), irradiation by UV, γ-rays, or ultrasonic waves (8–10), reduction with sodium naphthalenide (11), and catalytic hydrodechlorination (12–15), oxidation (16–19), or hydrolysis (20–22). Catalytic hydrolysis is the most practical way to treat CFC pollutants because of its use of nonnoble metal catalysts and readily available water, its high conversion, its simplicity, and its mild reaction conditions (20, 21). It also produces no dioxins. Compared with CFC oxidation in the absence of water vapor, the presence of water vapor in the reaction system can suppress the transformation of metal oxides in the catalysts to corresponding fluorides, thus increasing the selectivity and catalyst life (23, 24).

Many types of acid catalysts have been tried for the hydrolysis of CFCs. In general, they can be classified into two categories. (i) Fluorine nonresistant catalysts such as γ-Al_2O_3 (25), zeolites (26), heteropolyacids (27), and alumina-based catalysts (20, 28) decompose CFCs in the presence of water vapor at relatively high temperature and lose their activity rather quickly on stream due to surface fluorination. (ii) The activity of fluorine-resistant catalysts such as titania (23), titania- or zirconia-based catalysts (29–31), sulfated metal oxides (32–34), tungstated metal oxides (35–37), and metal phosphates (21, 38–41) for the hydrolysis of CCl_2F_2 varies, and it is difficult to make a precise comparison among these catalysts because of the different reaction conditions. Roughly speaking, complete hydrolysis of CCl_2F_2 in the presence of water vapor occurs on the catalysts from 250 to 450°C. The catalytic stability of these catalysts on stream is much better than that of the catalysts in the first category, because surface fluorination either hardly takes place or is not as severe as that for the first category.

It is well known that a fair amount of medium-strong acid sites are generated on the surfaces of many metal sulfates after calcination (42, 43). As a result, they are active for various reactions such as hydration, dehydration, alkylation, isomerization, esterification, and polymerization. In this work, catalytic hydrolysis of CCl_2F_2 over a series of metal sulfates was studied. Among them titanyl sulfate was found to be the most effective catalyst for the reaction. Moreover, titanyl sulfate was supported on nanosized titania prepared

[1] To whom correspondence should be addressed. Fax: 86-21-65641740. E-mail: zigao@fudan.edu.cn.

0021-9517/01 $35.00

by different methods, and the activity, selectivity, and stability of the supported catalysts were investigated in detail.

EXPERIMENTAL

Catalyst Preparation

The original metal sulfates used in this work were hydrated $Ti(SO_4)_2$, $SnSO_4$, $Al_2(SO_4)_3$, $NiSO_4$, $Fe_2(SO_4)_3$, $MnSO_4$, $CaSO_4$, and $CuSO_4$. They were dehydrated at 350°C for 3 h and pulverized. Then the dehydrated sulfate powder was calcined at 350°C for 3 h, except that $Ti(SO_4)_2$ was calcined at 350–650°C for 3 h to investigate the effect of calcination temperature on $Ti(SO_4)_2$.

$Ti(OH)_4$ was obtained by a conventional sol–gel method that involved the hydrolysis of $TiCl_4$ with ammonium hydroxide followed by aging, washing, and drying at 110°C. Titania-supported titanyl sulfate was prepared by an impregnation method (44). Upon mixing $Ti(SO_4)_2$ precalcined at 350°C with water, a gel-like material was obtained. $Ti(OH)_4$ was added to this slurry, followed by stirring, evaporating water, and drying at 110°C. The final calcination was carried out at various temperatures (400–700°C) for 3 h. The nonsupported and supported catalysts were labeled as TS-*t* and TS/TiO_2(*n*)-*t*, where *n* stood for the ratio of $TiOSO_4$ to TiO_2 in gram per gram and *t* for the calcination temperature in °C.

For comparison, three other kinds of TiO_2 with different structural and textural properties were also used as supports. A thermally stable mesoporous TiO_2 (m-TiO_2) with a nanosized anatase crystalline framework and ordered large pores was synthesized from a reaction mixture of 0.05 Ce^{3+}:1.0 TEOT:0.02 $EO_{20}PO_{70}EO_{20}$:4.0 H_2O:15.5 C_2H_5OH by stirring at ambient temperature for 48 h, followed by a hydrothermal process at 120°C for 24 h (45). Another kind of nanosized anatase TiO_2 (s-TiO_2) was prepared by a combination of sol–gel hydrolysis precipitation of titanium butoxide ($Ti(OC_4H_9)_4$) and hydrothermal treatment at 80°C for 24 h (46). A commercial crystalline TiO_2 (c-TiO_2) was obtained from the Chinese Medicine Company. Titanyl sulfate was loaded on these supports using the same impregnation method described previously. These catalysts were labeled as TS/m-TiO_2(*n*)-*t*, TS/s-TiO_2(*n*)-*t*, and TS/c-TiO_2(*n*)-*t* as stated earlier.

Catalyst Characterization

The crystallographic phases present in the catalysts were examined by X-ray diffraction (XRD). A Rigaku D/MAX-II X-ray diffractometer with a Cu$K\alpha$ X-ray source, a scan speed of 8°/min, and a scan range of 10–80° was used. The surface areas of the catalysts were measured by nitrogen adsorption at 77 K using a Micromeritics ASAP 2000 instrument and calculated by the BET method. The amount of acid sites was measured by NH_3 temperature-programmed desorption (NH_3-TPD) in a flow-type fixed-bed reactor at ambient pressure. The sample (0.1 g) was heated at 300°C for 3 h and cooled to 120°C in flowing He. At this temperature, the sample was treated by sufficient pulses of NH_3 until adsorption saturation, followed by a He purge for about 2 h. The temperature was then raised up from 120 to 300°C at a rate of 10°C/min to desorb NH_3 and was further maintained at 300°C for 1 h. The amount of acid sites estimated from the amount of NH_3 desorbed up to 300°C was defined as weak acid sites. The temperature was then raised up from 300 to 500°C and held at 500°C for 1 h. The amount of acid sites estimated from the amount of NH_3 desorbed between 300 and 500°C was defined as medium-strong acid sites. The sulfur content of the catalysts was detected by a chemical method. Dehydrated Na_2CO_3 and ZnO were used as fusing agents, and the sulfate was turned into $BaSO_4$ and determined by a gravimetric method.

Reaction Testing

The catalytic hydrolysis of CCl_2F_2 was carried out in a continuous fixed-bed flow microreactor under atmospheric pressure. CCl_2F_2 (1000 ppm), water vapor (6000 ppm), and balance air were mixed and passed through 0.4 g (40–60 mesh) of the catalyst at a space velocity (GHSV) of 10,000 h^{-1}. Effluent gases were passed through a KOH solution to eliminate the HF and HCl produced during the reaction. Before the KOH trap, gases were collected and identified using a gas chromatograph equipped with a thermal conductance detector (TCD). The main hydrolysis product was CO_2 and no CO by-product was detected for all the catalysts. Unreacted CCl_2F_2 and another possible $CClF_3$ by-product were separated with an Apiezon grease L/SiO_2 column (0.7 m) at 70°C and then analyzed by a gas chromatograph equipped with a flame ionization detector (FID). The conversion of CCl_2F_2 and selectivity to $CClF_3$ were calculated as follows:

$$[\text{Conversion of } CCl_2F_2] = ([CCl_2F_2]_{in} - [CCl_2F_2]_{out})/[CCl_2F_2]_{in} \times 100\%;$$

$$[\text{Selectivity to } CClF_3] = [CClF_3]_{out}/([CCl_2F_2]_{in} - [CCl_2F_2]_{out}) \times 100\%,$$

where $[\ ]_{in}$ and $[\ ]_{out}$ meant the concentration of the chemical substance going into and coming out from the reactor.

RESULTS

Activity of Metal Sulfates

The activities of various dehydrated metal sulfates for the hydrolysis of CCl_2F_2 were tested and depicted in Fig. 1 as a function of reaction temperature. Among all the sulfates, titanium sulfate showed the highest activity. CCl_2F_2

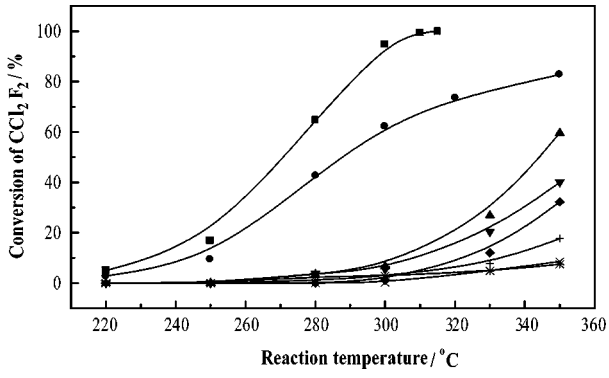

FIG. 1. CCl_2F_2 conversion on metal sulfates as a function of reaction temperature. Reaction mixture: 1000 ppm CCl_2F_2 and 6000 ppm water vapor in air. Catalyst: 0.4 g. ■—$Ti(SO_4)_2$, ●—$SnSO_4$, ▲—$Al_2(SO_4)_3$, ▼—$NiSO_4$, ◆—$Fe_2(SO_4)_3$, +—$MnSO_4$, ×—$CuSO_4$, ✳—$CaSO_4$.

began to decompose above 200°C and the conversion increased rapidly with reaction temperature. Complete conversion of CCl_2F_2 was reached at 310°C. No CO and $CClF_3$ were formed during the reaction. Stannous sulfate showed the next highest activity for the hydrolysis of CCl_2F_2. The conversion on $SnSO_4$ reached 84.5% at 350°C. The catalytic activities of all the other metal sulfates were lower, converting less than 60% of CCl_2F_2 at 350°C. The activity sequence of the anhydrous metal sulfates is $Ti(SO_4)_2$ > $SnSO_4$ > $Al_2(SO_4)_3$ > $NiSO_4$ > $Fe_2(SO_4)_3$ > $MnSO_4$ > $CaSO_4$, $CuSO_4$.

The electronegativity and specific surface area of the metal sulfates are listed in Table 1. No simple relation between the activity and these parameters could be found. It has been noted that electronegativity is an important parameter of metal sulfates determining their activity and selectivity in acid-catalyzed reactions (47–49). However, in some of the reactions conducted on unsupported metal sulfates, such as dehydration of ethanol, a simple relationship between activity and electronegativity does not exist. Such a phenomenon has been explained by the difference in surface area from one dehydrated metal sulfate to another (49). From the results in Table 1, this explanation is also questionable. The failure to find a clear correlation between activity and electronegativity and/or surface area here may result from the complexity of the variation in the concentration and reactivity of the surface acid sites connected to the extent of dehydration of the metal sulfates. Since the formation of acid sites on metal sulfates is related to the generation of vacant sites in the sulfate structure upon dehydration, the acidic properties of metal sulfates depend greatly on their degree of dehydration (43). In our experiments, the degree of dehydration of the sulfates upon calcination at 350°C and the degree of their rehydration during the reaction vary from one to another; hence it is not surprising that the order of activity for CCl_2F_2 hydrolysis does not parallel with that based on electronegativity and/or specific surface area.

TABLE 1

Activity and Properties of Metal Sulfates

Sulfate	Conversion of CCl_2F_2 (%) 270°C	310°C	350°C	χ_i[a]	Surface area (m^2/g)
Ti(IV)	48.4	100	—	13.5	7.9
Sn(II)	32.1	69.7	84.5	9.0	9.8
Al(III)	2.4	13.9	59.6	10.5	3.0
Ni(II)	2.0	10.4	40.0	9.0	28
Fe(III)	0	4.6	32.2	12.6	5.3
Mn(II)	0	4.2	17.6	7.5	4.9
Ca(II)	0	3.2	7.5	5.0	10
Cu(II)	0	1.5	8.5	9.5	11

[a] $\chi_i = (1 + 2Z)\chi_0$, χ_0 is the electronegativity of the neutral atom given by Pauling, and Z is the charge of the ion (47).

Since titanium sulfate is the most efficient catalyst for the reaction, the following experiments were conducted mainly on this particular sulfate.

Effect of Calcination Temperature

As shown in Fig. 2, the activity of titanium sulfate decreased with increasing calcination temperature. CCl_2F_2 was decomposed completely at 310°C on TS-350, whereas TS-650 decomposed CCl_2F_2 completely at 375°C, close to the complete decomposition temperature of pure TiO_2. Catalytic activities of $Ti(SO_4)_2$ calcined at different temperatures for cumene cracking at 180°C were reported and the maximum activity was observed with calcination at 625°C (50). The inconsistency of the optimum calcination temperature in these two cases suggests that the acid strengths of the acid sites required for the two reactions are different. Cumene cracking at low temperature is catalyzed only by very strong acid sites, but medium-strong acid sites are needed for the catalytic hydrolysis of CCl_2F_2 (39).

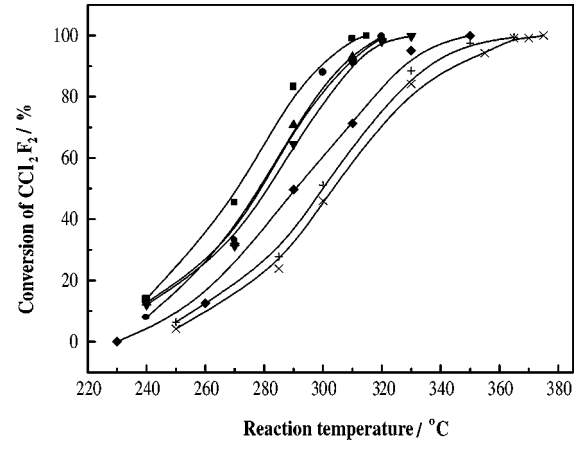

FIG. 2. CCl_2F_2 conversion on TS-*t* series as a function of reaction temperature. Reaction mixture: 1000 ppm CCl_2F_2 and 6000 ppm water vapor in air. Catalyst: 0.4 g. ■—TS-350, ●—TS-400, ▲—TS-450, ▼—TS-500, ◆—TS-550, +—TS-600, ×—TS-650.

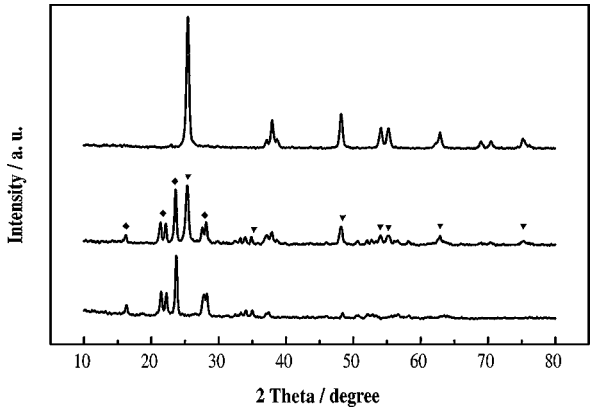

FIG. 3. XRD patterns of TS-*t* series. From bottom to top: TS-350, TS-600, TS-650. ◆—$TiOSO_4$, ▼—anatase TiO_2.

XRD patterns of $Ti(SO_4)_2$ calcined at 350, 600, and 650°C are shown in Fig. 3. Only diffractions of $TiOSO_4$ were observed in the pattern of the sample calcined at 350°C. Strong diffraction peaks of both anatase TiO_2 and $TiOSO_4$ appeared in the sample calcined at 600°C, and the diffraction peaks of $TiOSO_4$ disappeared in the sample calcined at 650°C. These results imply that titanyl sulfate provides the medium-strong acid sites active for the hydrolysis of CCl_2F_2, and the activity of the catalyst is correlated with the amount of $TiOSO_4$ in the catalyst. In contrast, the very strong acid sites active for cumene cracking at low temperature reported in the literature may result from further decomposition of $TiOSO_4$ above 350°C, when the catalyst has partly transformed to anatase TiO_2. As the calcination temperature was further increased to 650°C, desulfation of the catalyst was almost completed, and so the activities for both reactions dropped.

To improve the activity of titanyl sulfate, it was supported on titania prepared by a conventional sol–gel method. Figure 4 illustrates the CCl_2F_2 hydrolysis activities of TS/TiO_2(0.2)-*t* series catalysts calcined at different temperatures. Obviously, the optimum calcination temperature for the series with the same titanyl sulfate loading of 0.2 g/g was 500 instead of 350°C. CCl_2F_2 was decomposed over TS/TiO_2(0.2)-500 completely at 265°C, which was 45°C lower than the complete hydrolysis temperature of the nonsupported TS-350 catalyst. Both TS/TiO_2(0.2)-400 and TS/TiO_2(0.2)-600 were less active than TS/TiO_2(0.2)-500. Complete conversion of CCl_2F_2 was reached on these catalysts around 300°C, which was still slightly lower than the complete hydrolysis temperature of TS-350. Meanwhile, the calcination temperature of 700°C was definitely too high for the supported catalyst due to desulfation. The catalytic performance of TS/TiO_2(0.2)-700 became similar to that of the TiO_2 support, converting CCl_2F_2 completely above 360°C.

It was noted during reaction tests that the activity of TS/TiO_2(0.2)-400 and TS/TiO_2(0.2)-500 reached steady state within 15 min under all reaction temperatures, whereas for the other three catalysts the steady-state activity was reached after more than 1 h on stream, as shown in Fig. 5. The initial increase in activity for these catalysts is probably related to the surface fluorination of TiO_2 at high reaction temperatures (23, 32). A fluorine substitution mechanism for the TiO_2 catalyst has been proposed to explain the generation of additional acid sites responsible for the increase in activity (23). When fluorine replaces the surface hydroxyl attached to Ti^{4+}, fluorine pulls the electrons in the adjacent bonds toward itself and consequently the adjacent O–H bond is weakened, making the hydrogen more acidic. For TS/TiO_2(0.2)-400 and TS/TiO_2(0.2)-500 catalysts, surface fluorination of the catalysts is inhibited because of their high surface sulfate content and low reaction temperature.

XRD patterns of TS/TiO_2(0.2)-*t* series catalysts are shown in Fig. 6. Only diffractions of anatase TiO_2 were

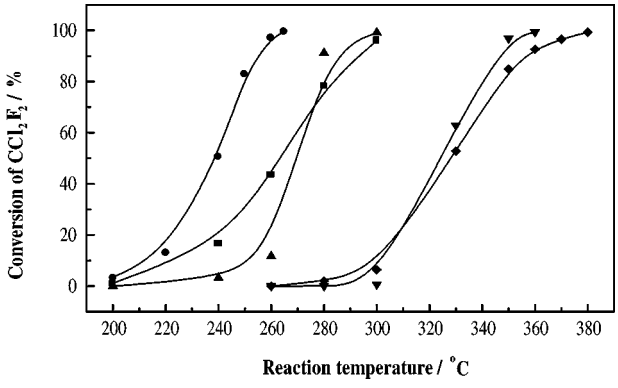

FIG. 4. CCl_2F_2 conversion on the TS/TiO_2(0.2)-*t* series as a function of reaction temperature. Reaction mixture: 1000 ppm CCl_2F_2 and 6000 ppm water vapor in air. Catalyst: 0.4 g. ■—TS/TiO_2(0.2)-400, ●—TS/TiO_2(0.2)-500, ▲—TS/TiO_2(0.2)-600, ▼—TS/TiO_2(0.2)-700, ◆—TiO_2-500.

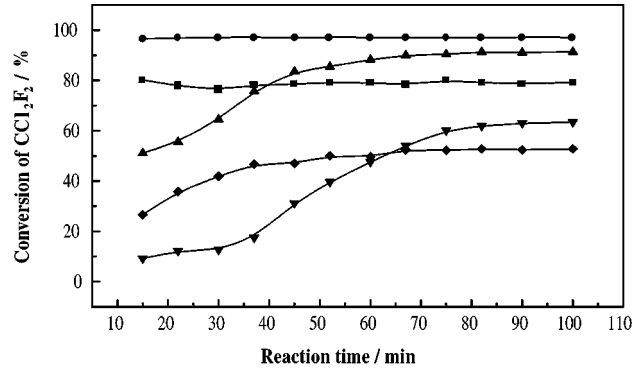

FIG. 5. CCl_2F_2 conversion of TS/TiO_2(0.2)-*t* series as a function of reaction time. Reaction mixture: 1000 ppm CCl_2F_2 and 6000 ppm water vapor in air. Catalyst: 0.4 g. ■—TS/TiO_2(0.2)-400 (280°C), ●—TS/TiO_2(0.2)-500 (260°C), ▲—TS/TiO_2(0.2)-600 (280°C), ▼—TS/TiO_2(0.2)-700 (330°C), ◆—TiO_2-500 (330°C).

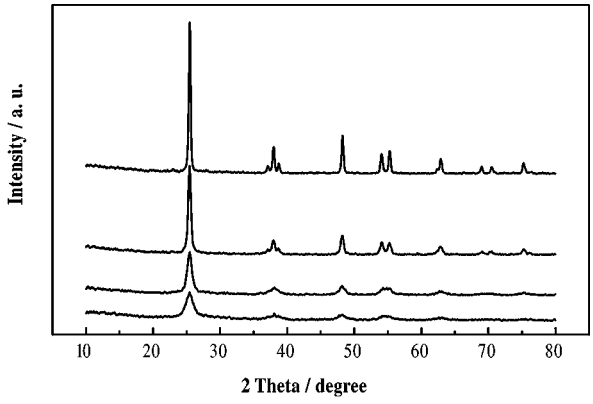

FIG. 6. XRD patterns of TS/TiO_2(0.2)-*t* series. From bottom to top: TS/TiO_2(0.2)-400, TS/TiO_2(0.2)-500, TS/TiO_2(0.2)-600, TS/TiO_2(0.2)-700.

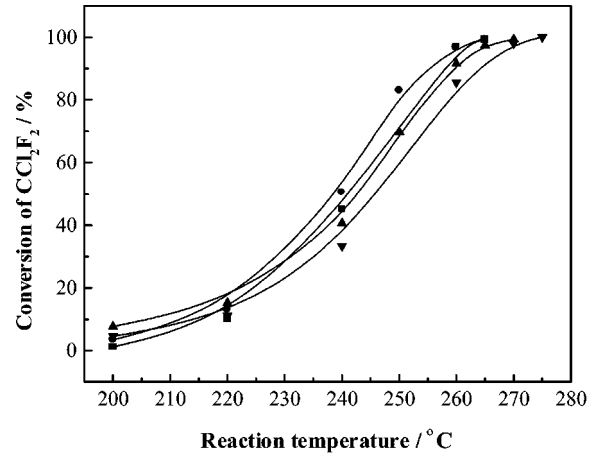

FIG. 7. CCl_2F_2 conversion on the TS/TiO_2(*n*)-500 series as a function of reaction temperature. Reaction mixture: 1000 ppm CCl_2F_2 and 6000 ppm water vapor in air. Catalyst: 0.4 g. ■—TS/TiO_2(0.1)-500, ●—TS/TiO_2(0.2)-500, ▲—TS/TiO_2(0.4)-500, ▼—TS/TiO_2(0.6)-500.

observed in the patterns due to the high dispersion of titanyl sulfate on TiO_2 support. The intensity of the diffraction peaks increases with calcination temperature, implying that the crystallite size of TiO_2 is increased. The sulfur content, specific surface area, crystallite size calculated from the Scherrer equation, and amount of acid sites determined by the NH_3-TPD method of the TS/TiO_2(0.2)-*t* series catalysts are summarized in Table 2. The sulfur content, specific surface area, and total amount of acid sites of the catalysts decrease monotonicly with calcination temperature, while the crystallite size of anatase TiO_2 increases. The high surface area and surface acidity of the catalysts calcined below 600°C are responsible for their high activity toward CCl_2F_2 hydrolysis. On the other hand, TS/TiO_2(0.2)-500 has more medium-strong acid sites than the other catalysts, which explains its maximal activity for CCl_2F_2 hydrolysis in the series.

Effect of Titanyl Sulfate Loading

As the ratio of $TiOSO_4/TiO_2$ increased from 0.1 to 0.6 g/g, the activity of the TS/TiO_2(*n*)-500 series showed slight changes, as shown in Fig. 7. Complete conversion of CCl_2F_2 over TS/TiO_2(0.1)-500, TS/TiO_2(0.2)-500, TS/TiO_2(0.4)-500, and TS/TiO_2(0.6)-500 occurred at 265, 265, 270, and 275°C, respectively.

The XRD patterns of the TS/TiO_2(*n*)-500 series are given in Fig. 8. Broad diffraction peaks of anatase TiO_2 were observed for all the samples, implying that the crystallites of TiO_2 in the catalysts were nanosized. No $TiOSO_4$ diffraction peaks were found for samples with $TiOSO_4/TiO_2$ ratios below 0.2 g/g, indicating that the sulfate was highly dispersed on the support. For the sample with a $TiOSO_4/TiO_2$ ratio of 0.4 g/g, a weak diffraction peak ($2\theta = 28°$) of $TiOSO_4$ was observed. The intensity of the diffraction peaks of $TiOSO_4$ increased further with an increasing $TiOSO_4/TiO_2$ ratio. The specific surface area of the catalysts and the crystallite size of TiO_2 in the catalysts calculated from the Scherrer equation are listed in Table 3. The crystallite sizes of anatase TiO_2 in the catalysts are much smaller than those in pure TiO_2 calcined at the same temperature, so that the surface areas of the catalysts are considerably higher than those in pure TiO_2. This shows that dispersion of titanyl sulfate on TiO_2 inhibits the growth of anatase crystallites significantly during calcination. The slight decrease in catalytic activity for samples with loading of titanyl sulfate above 0.4 g/g may result from the reduction in surface area with increasing loading.

TABLE 2

Physical and Chemical Properties of TS/TiO_2(0.2)-*t* Series Catalysts

Calcination temperature (°C)	SO_3 content (wt%)	Surface area (m^2/g)	Crystallite size (nm)	Weak acid sites (mmol/g)	Medium-strong acid sites (mmol/g)	Total acid sites (mmol/g)
400	10.0	129	12	0.910	0.265	1.175
500	6.6	100	18	0.705	0.292	0.997
600	1.7	47	40	0.541	0.165	0.706
700	0.9	17	240	0.327	0.107	0.434

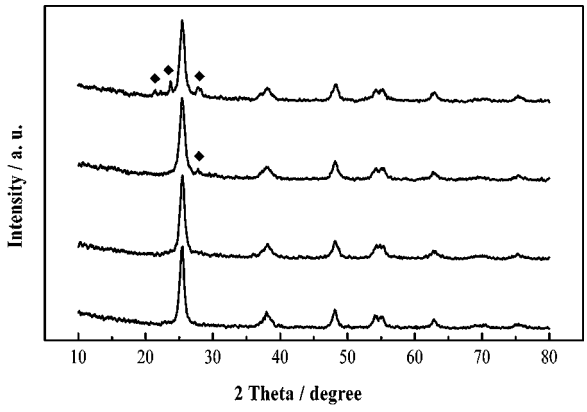

FIG. 8. XRD patterns of TS/TiO_2(*n*)-500 series. From bottom to top: TS/TiO_2(0.1)-500, TS/TiO_2(0.2)-500, TS/TiO_2(0.4)-500, TS/TiO_2(0.6)-500. ◆—$TiOSO_4$.

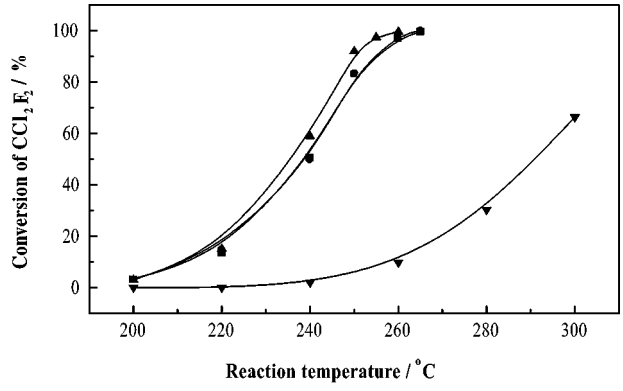

FIG. 9. CCl_2F_2 conversion of titanyl sulfate supported on various TiO_2 as a function of reaction temperature. Reaction mixture: 1000 ppm CCl_2F_2 and 6000 ppm water vapor in air. Catalyst: 0.4 g. ■—TS/TiO_2(0.2)-500, ●—TS/s-TiO_2(0.2)-500, ▲—TS/m-TiO_2(0.2)-500, ▼—TS/c-TiO_2(0.2)-500.

Effect of Various TiO_2 Supports

There are numerous ways to prepare nanosized TiO_2. The most common method is sol–gel hydrolysis precipitation followed by calcination (51) or hydrothermal treatment (46). The latter was known to be an effective method to promote crystallization of titania under mild temperatures and to produce a nanocrystalline titania of ultrahigh surface area. Hence, in this work nanosized anatase TiO_2 support (s-TiO_2) was prepared following the procedure described in the literature (46). Recently, a mesoporous TiO_2 with a nanosized crystalline anatase TiO_2 framework (m-TiO_2) was synthesized successfully using a block copolymer $EO_{20}PO_{70}EO_{20}$ as a structure-directing agent in our laboratory (45). This type of material has a high specific surface area (≈150 m^2/g), a large pore size (≈6 nm), and a regular pore structure, which are essential to a good catalyst support. Titanyl sulfate was loaded on s-TiO_2, m-TiO_2, and a commercial TiO_2 (c-TiO_2), and the activities of these catalysts for CCl_2F_2 hydrolysis were compared.

Figure 9 shows the temperature profiles of CCl_2F_2 hydrolysis on titanyl sulfate supported on various types of TiO_2. Among the catalysts, TS/m-TiO_2(0.2)-500 exhibited the highest activity. Complete hydrolysis of CCl_2F_2 occurred at 260°C, which was even lower than the complete hydrolysis temperature (265°C) of TS/s-TiO_2(0.2)-500 and TS/TiO_2(0.2)-500. TS/c-TiO_2(0.2)-500 was the least active catalyst. It was almost inactive for the reaction below 240°C, and the conversion of CCl_2F_2 on the catalyst was only about 10% at 260°C.

XRD patterns of these supported titanyl sulfate catalysts are given in Fig. 10. Similar to TS/TiO_2(0.2)-500, only broad diffractions of anatase TiO_2 were observed in the patterns of TS/m-TiO_2(0.2)-500 and TS/s-TiO_2(0.2)-500, indicating that titanyl sulfate was also highly dispersed on these nanosized anatase TiO_2 supports. Sharp diffraction peaks of anatase TiO_2 and relatively weak peaks of rutile TiO_2 were observed in TS/c-TiO_2(0.2)-500. The specific surface area and crystallite size of anatase TiO_2 calculated from the Scherrer equation of the catalysts are listed in Table 4. The variation of activity among these catalysts correlates well with their difference in surface area, showing that

TABLE 3

Properties of TS/TiO_2(*n*)-500 Series Catalysts

Catalysts	Surface area (m^2/g)	Crystallite size (nm)
TS/TiO_2(0.1)-500	84	21
TS/TiO_2(0.2)-500	100	18
TS/TiO_2(0.4)-500	79	14
TS/TiO_2(0.6)-500	68	14
TiO_2-500	16	200

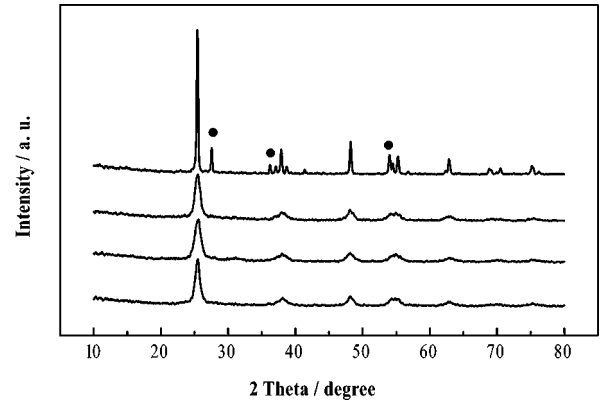

FIG. 10. XRD patterns of titanyl sulfate supported on various TiO_2's. From bottom to top: TS/TiO_2(0.2)-500, TS/m-TiO_2(0.2)-500, TS/s-TiO_2(0.2)-500, TS/c-TiO_2(0.2)-500. ●—rutile TiO_2

TABLE 4

Properties of Various Supported Titanyl Sulfate Catalysts

Catalysts	Surface area (m^2/g)	Crystallite size (nm)
TS/m-TiO_2(0.2)-500	111	13
TS/s-TiO_2(0.2)-500	103	15
TS/c-TiO_2(0.2)-500	8.0	—
TS/TiO_2(0.2)-500	100	18

increasing the surface area of the titania-supported catalyst is advantageous to the reaction.

Catalyst Stability

TS/TiO_2(0.2)-500 was chosen as a representative sample to test the catalytic stability of this type of catalyst. To clarify the changes in activity with time, the test was carried out at 260°C because the conversion of CCl_2F_2 would not reach 100% under this condition. The result is shown in Fig. 11, and no deactivation was observed on TS/TiO_2(0.2)-500 within the test period. The initial conversion was 96.9%, and it remained unchanged after 360 h on stream. Again, no CO was detected in the effluent gas, and the selectivity to $CClF_3$ is shown in Fig. 11. The amount of $CClF_3$ detected in the effluent did not exceed 0.5% in the whole reaction course of 360 h.

XRD patterns of the catalyst before and after reaction are compared in Fig. 12. No obvious structural change of the catalyst could be found. The surface area and sulfur content of the catalyst after reaction were 86.8 m^2/g and 6.4 wt%, respectively, which were a little lower than those of the fresh catalyst (see Table 2). The previous results demonstrate that TS/TiO_2(0.2)-500 is not only active and selective for the complete hydrolysis of CCl_2F_2 in the presence of water vapor but also very stable on stream, implying that the catalyst is rather inert toward the gaseous products HF and HCl formed in the reaction.

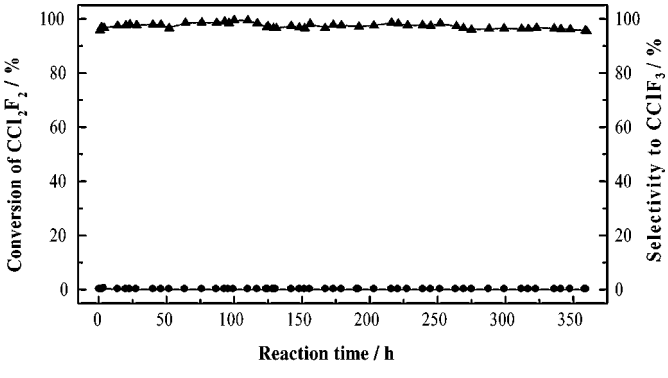

FIG. 11. Activity and selectivity of TS/TiO_2(0.2)-500 on stream. Reaction mixture: 1000 ppm CCl_2F_2 and 6000 ppm water vapor in air. Catalyst: 0.4 g. ▲—Conversion of CCl_2F_2, ●—selectivity to $CClF_3$.

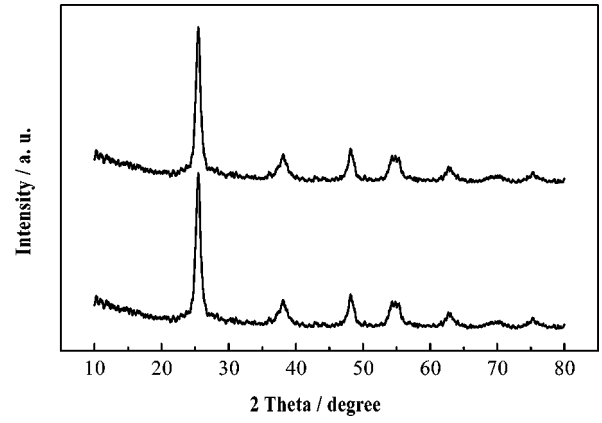

FIG. 12. XRD patterns of TS/TiO_2(0.2)-500 before and after reaction. From bottom to top: TS/TiO_2(0.2)-500 before reaction, TS/TiO_2(0.2)-500 after reaction.

DISCUSSION

The major reaction of CCl_2F_2 hydrolysis in the presence of water vapor and air is (39)

$$CCl_2F_2 + 2H_2O \rightarrow CO_2 + 2HF + 2HCl.$$

Based on *in situ* IR results, the following reaction mechanism has been proposed (23):

$$CX_4 + H^+ \rightarrow CX_4H^+ \quad X = Cl,\ F$$
$$CX_4H^+ + OH^- \rightarrow COX_2 + 2HX$$
$$COX_2 + H_2O \rightarrow CO_2 + 2HX.$$

Adsorption of CCl_2F_2 molecules on Brønsted acid sites with simultaneous reaction between CCl_2F_2 and surface hydroxyls is probably the rate-determining step, when the concentration of water vapor in the feed is in excess, so that the activity of the catalysts depends on the amount of acid sites on the catalyst surface. Meanwhile, $CClF_3$ may form in the reaction as a minor by-product through halogen exchange on the catalyst,

$$CCl_2F_2 + F^- \rightarrow CClF_3 + Cl^-.$$

Strong acid sites could abstract F^- from CCl_2F_2, leading to an increase in the concentration of F^- on the catalyst surface and enhancing the formation of $CClF_3$ (39). Therefore, catalysts abundant in medium-strong acid sites, such as $TiOSO_4$ formed by calcination of titanium sulfate at an appropriate temperature, are more ideal for complete and selective hydrolysis of CCl_2F_2.

Hydrogen fluoride formed in the hydrolysis of CCl_2F_2 is extremely corrosive. Alumina, zeolites, and many other acid catalysts will deteriorate during reaction due to surface fluorination. Chemical compounds with smaller negative Gibbs free energy changes for their reaction with HF should be more resistant to fluorination (39, 51). The ΔG values of the

TABLE 5

ΔG Values of the Formation of Fluoride from Metal Oxides, Phosphates, and Sulfates

Oxide	ΔG (kJ/mol)	Phosphate	ΔG (kJ/mol)	Sulfate	ΔG (kJ/mol)
MgO	−96.3	$Mg_3(PO_4)_2$	−43.1	$MgSO_4$	−27.0
CaO	−123.0	$Ca_3(PO_4)_2$	−33.5	$CaSO_4$	+1.3
γ-Al_2O_3	−57.4	$AlPO_4$	−35.0	$Al_2(SO_4)_3$	−34.0
Fe_2O_3	−40.9	$FePO_4$	—	$Fe_2(SO_4)_3$	−18.2
NiO	−37.3	$Ni_3(PO_4)_2$	−7.3	$NiSO_4$	+6.0
CuO	−25.8	$Cu_3(PO_4)_2$	−5.0	$CuSO_4$	+9.6
a-TiO_2	−10.1	—	—	—	—

formation of metal fluorides from metal oxides, phosphates, and sulfates were calculated using the few thermodynamic data available in the handbook (53) and are listed in Table 5. It is obvious that the calculated ΔG values of metal sulfates are less negative than those of metal oxides and phosphates and in some cases the ΔG values even become positive. This explains the superiority of metal sulfates over metal oxides and phosphates in the aspect of antifluorination during reaction. Therefore, it is not surprising to find that catalysts composed of metal sulfate have a longer catalyst life than the other catalysts. In addition to this, the ΔG value of fluoride formation of anatase TiO_2 is less negative compared to those of the other metal oxides, so that anatase TiO_2 is an ideal supporting material for CCl_2F_2 hydrolysis catalysts.

A high specific area is one of the essential requirements for an active catalyst. The specific surface area of $TiOSO_4$ formed by calcination of titanium sulfate at 350°C is only 7.9 m^2/g, which is indeed rather small for a practical catalyst. Supporting $TiOSO_4$ on nanosized anatase TiO_2 is an effective way to increase the specific surface area of the catalyst to around 100 m^2/g and to improve its catalytic activity. In the present work, nanosized titania-supported titanyl sulfate catalysts have been prepared successfully in two ways. One is a two-step method, i.e., preparing a nanosized anatase TiO_2 support first and then supporting $TiOSO_4$ on it by impregnating and calcining at 500°C, such as the preparation methods of TS/m-TiO_2(0.2)-500 and TS/s-TiO_2(0.2)-500. The other is a one-step method, i.e., impregnating $TiOSO_4$ directly on amorphous $Ti(OH)_4$ and calcining at 500°C, such as the method used for TS/TiO_2(0.2)-500. It has been observed that there is no significant difference in the structure and specific surface area of the catalysts prepared in these two ways, and so their activity and selectivity for the hydrolysis of CCl_2F_2 are close to each other. Experimental results in this work show that dispersion of $TiOSO_4$ on amorphous titania promotes the formation of nanosized anatase TiO_2 and inhibits its crystal growth during calcination, so that the crystallite size of anatase TiO_2 in TS/TiO_2(0.2)-500 is much smaller than that in TiO_2-500 and only slightly larger than that in TS/m-TiO_2(0.2)-500 and TS/s-TiO_2(0.2)-500 (see Tables 3 and 4). On the other hand, the dispersion of $TiOSO_4$ also inhibits the phase transition of the nanosized anatase TiO_2 in the catalysts. Hence, no rutile phase has appeared in the catalysts calcined at 500–600°C, which helps the catalysts to maintain their large surface area and high catalytic activity for the hydrolysis of CCl_2F_2.

CONCLUSIONS

The hydrolysis of CCl_2F_2 in the presence of water vapor and air was studied over various metal sulfates. Among these sulfates, $TiOSO_4$ formed by calcination of titanium sulfate at 350°C is the most active catalyst for the reaction. The complete hydrolysis temperature of CCl_2F_2 on $TiOSO_4$ is 310°C. Supporting $TiOSO_4$ on nanosized anatase TiO_2 may further increase its activity. CCl_2F_2 decomposes completely on nanosized titania-supported $TiOSO_4$ catalysts at 260–265°C. The activity of the supported catalysts correlates well with their specific surface area and the amount of medium-strong acid sites on the surface. The results of a 360-h long-term experiment show that the activity of the supported catalyst is very stable and the selectivity to $CClF_3$ in the effluent remains lower than 0.5%. This supported $TiOSO_4$ catalyst promises to be of practical use.

ACKNOWLEDGMENTS

This work was supported by the Major State Basic Research Development Program (Grant 2000077500) and the Foundation for University Key Teacher by the Ministry of Education.

REFERENCES

1. Molina, M. J., and Rowland, F. S., *Nature* **249**, 810 (1974).
2. Graham, J. L., Hall, D. L., and Dellinger, B., *Environ. Sci. Technol.* **20**, 703 (1986).
3. Sudo, K., Sakae, K., Hirose, T., Takahashi, H., and Miyakoshi, T., *Chichibu-Onoda Rep.* **47**, 96 (1996).
4. Spiess, F. J., Chen, X., Brock, S. L., Suib, S. L., Hayashi, Y., and Matsumoto, H., *J. Phys. Chem. A* **104**, 11,111 (2000).
5. Sugeta, T., Japan Patent kokal 274, 269 (1990).
6. Sonoyama, N., and Sakata, T., *Environ. Sci. Technol.* **32**, 375 (1998).
7. Sonoyama, N., and Sakata, T., *Environ. Sci. Technol.* **32**, 4005 (1998).
8. Jo, S. K., and White, J. M., *Surf. Sci.* **245**, 305 (1991).
9. Nagata, Y., Hirai, K., Okitsu, K., Dohmaru, T., and Maeda, Y., *Chem. Lett.* 203 (1995).
10. Yamamoto, Y., and Tagawa, S., *Chem. Lett.* 477 (1998).
11. Oku, A., Kimura, K., and Sato, M., *Ind. Eng. Chem. Res.* **28**, 1055 (1989).
12. Karpinski, Z., Early, K., and d'Itri, J. L., *J. Catal.* **164**, 378 (1996).
13. Wiersma, A., Van de Sandt, E. J. A. X., den Hollander, M. A., Makkee, M., Van Bekkum, H., and Moulijn, J. A., *J. Catal.* **177**, 29 (1998).
14. Early, K., Kovalchuk, V. I., Lonyi, F., Deshmukh, S., and d'Itri, J. L., *J. Catal.* **182**, 219 (1999).
15. Ordonez, S., Makkee, M., and Moulijn, J. A., *Appl. Catal. B* **29**, 13 (2001).
16. Imamura, S., Shiomi, T., Ishida, S., Utani, K., and Jindai, H., *Ind. Eng. Chem. Res.* **29**, 1758 (1990).
17. Imamura, S., *Catal. Today* **11**, 547 (1992).

18. Karmakar, S., and Greene, H. L., *J. Catal.* **138**, 364 (1992).
19. Karmakar, S., and Greene, H. L., *J. Catal.* **148**, 524 (1994).
20. Okazaki, S., and Kurosaki, A., *Chem. Lett.* 1901 (1989).
21. Takita, Y., *Shokubai* (*Catalyst*) **41**, 284 (1999).
22. Ma, Z., Hua, W. M., and Gao, Z., *Chin. Bull. Chem.* **64**, 339 (2001).
23. Karmakar, S., and Greene, H. L., *J. Catal.* **151**, 394 (1995).
24. Takita, Y., and Ishihara, T., *Catal. Surv. Jpn.* **2**, 165 (1998).
25. Nagata, H., Takakura, T., Tashiro, S., Kishida, M., Mizuno, K., Tamori, I., and Wakabayashi, K., *Appl. Catal. B* **5**, 23 (1994).
26. Tajima, M., Niwa, M., Fujii, Y., Koinuma, Y., Aizawa, R., Kushiyama, S., Kobayashi, S., Mizuno, K., and Ohuchi, H., *Appl. Catal. B* **9**, 167 (1996).
27. Ma, Z., Hua, W. M., Tang, Y., and Gao, Z., *Chin. J. Catal.* **1**, 3 (2000).
28. Ng, C. F., Shan, S., and Lai, S. Y., *Appl. Catal. B* **16**, 209 (1998).
29. Bickle, G. M., Suzuki, T., and Mitarai, Y., *Appl. Catal. B* **4**, 141 (1994).
30. Tajima, M., Niwa, M., Fujii, Y., Koinuma, Y., Aizawa, R., Kushiyama, S., Kobayashi, S., Mizuno, K., and Ohuchi, H., *Appl. Catal. B* **12**, 263 (1997).
31. Tajima, M., Niwa, M., Fujii, Y., Koinuma, Y., Aizawa, R., Kushiyama, S., Kobayashi, S., Mizuno, K., and Ohuchi, H., *Appl. Catal. B* **14**, 97 (1997).
32. Fu, X. Z., Zeltner, W. A., Yang, Q., and Anderson, M. A., *J. Catal.* **168**, 482 (1997).
33. Lai, S. Y., Pan, W. X., and Ng, C. F., *Appl. Catal. B* **24**, 207 (2000).
34. Ma, Z., Hua, W. M., Tang, Y., and Gao, Z., *Chin. J. Chem.* **3**, 341 (2000).
35. Ma, Z., Hua, W. M., Tang, Y., and Gao, Z., *Chem. Lett.* 1215 (1999).
36. Ma, Z., M., Hua, W., Tang, Y., and Gao, Z., *J. Mol. Catal. A* **159**, 335 (2000).
37. Hua, W. M., Zhang, F., Ma, Z., Tang, Y., and Gao, Z., *Catal. Lett.* **65**, 85 (2000).
38. Takita, Y., Li, G. L., Matsuzaki, R., Wakamatsu, H., Nishiguchi, H., Moro-oka, Y., and Ishihara, T., *Chem. Lett.* 13 (1997).
39. Takita, Y., Ninomiya, M., Matsuzaki, R., Wakamatsu, H., Nishiguchi, H., and Ishihara, T., *Phys. Chem. Chem. Phys.* **1**, 2367 (1999).
40. Takita, Y., Wakamatsu, H., Li, G. L., Moro-oka, Y., Nishiguchi, H., and Ishihara, T., *J. Mol. Catal. A* **155**, 111 (2000).
41. Takita, Y., Wakamatsu, H., Tokumaru, M., Nishiguchi, H., Ito, M., and Ishihara, T., *Appl. Catal. A* **194–195**, 55 (2000).
42. Tanabe, K., and Takeshita, T., *Adv. Catal.* **17**, 315 (1967).
43. Takeshita, T., Ohnishi, R., and Tanabe, K., *Catal. Rev.* **8**, 29 (1973).
44. Huang, Y., Zhao, B., and Xie, Y., *Appl. Catal. A* **171**, 65 (1998).
45. Yue, Y., and Gao, Z., *Chem. Commun.* 1755 (2000).
46. Wang, C. C., and Ying, J. Y., *Chem. Mater.* **11**, 3113 (1999).
47. Tanaka, K. I., and Ozaki, A., *J. Catal.* **8**, 1 (1967).
48. Misono, M., Saito, Y., and Yoneda, Y., *J. Catal.* **9**, 135 (1967).
49. Mochida, I., Kato, A., and Seiyama, T., *J. Catal.* **22**, 23 (1971).
50. Arata, K., Hino, M., and Yamagata, N., *Bull. Chem. Soc. Jpn.* **63**, 244 (1990).
51. Cao, L., Huang, A., Spiess, F. J., and Suib, S. L., *J. Catal.* **188**, 48 (1999).
52. Li, G. L., Nishiguchi, H., Ishihara, T., Moro-oka, Y., and Takita, Y., *Appl. Catal. B* **16**, 309 (1998).
53. Dean, J. A., "Lange's Handbook of Chemistry" (thirteenth edition). McGraw–Hill, New York, 1985.